The Cryosphere Discuss., 3, 729–764, 2009
www.the-cryosphere-discuss.net/3/729/2009/

The Cryosphere Discussions

The Cryosphere Discussions is the access reviewed discussion forum of *The Cryosphere*

An efficient regional energy-moisture balance model for simulation of the Greenland ice sheet response to climate change

A. Robinson[1,2], R. Calov[1], and A. Ganopolski[1]

[1]Potsdam Institute for Climate Impact Research, Potsdam, Germany
[2]University of Potsdam, Potsdam, Germany

Received: 27 August 2009 – Accepted: 28 August 2009 – Published: 11 September 2009

Correspondence to: A. Robinson (robinson@pik-potsdam.de)

Published by Copernicus Publications on behalf of the European Geosciences Union.

Abstract

In order to explore the response of the Greenland ice sheet (GIS) to climate change on long (centennial to multi-millennial) time scales, a regional energy-moisture balance model has been developed. This model simulates seasonal variations of temperature and precipitation over Greenland and explicitly accounts for elevation and albedo feedbacks. These fields are used to force a high resolution ice sheet model through the annual mean surface temperature and mass balance. The melt component of the mass balance is computed here using both a conventional positive degree day approach and a more physically-based alternative. As a validation of the model, we first simulated temperature and precipitation over Greenland for the prescribed, present-day topography of Greenland and compared them with empirical data. For the present-day climate, simulated surface boundary conditions for the GIS do not differ significantly from those of a simple parameterization used in many previous simulations. However, for a prescribed, ice-free state, the differences in simulated climatology and surface mass balance between the regional energy-moisture balance model and the conventional approach become significant, with our model showing much stronger summer warming. When coupled to a high resolution, three-dimensional ice sheet model and initialized with present-day conditions, the two melt schemes both allow sufficiently realistic simulations of the present-day GIS. However, when starting from ice-free conditions, two different equilibrium states are achieved, depending on the choice of melt scheme.

1 Introduction

Modeling the future evolution of the Greenland ice sheet (GIS) has attracted considerable attention in recent years, due to a potentially significant contribution of the GIS to future sea level rise (Church et al., 2001). Over recent decades, observed significant mass losses of the GIS have been diagnosed by different methods (Abdalati and Steffen, 2001; Box et al., 2006; Rignot and Kanagaratnam, 2006; Rignot et al., 2008).

While it is expected that only a rather small portion of the GIS can melt over the 21st century, modeling studies (Huybrechts and de Wolde, 1999; Ridley et al., 2005; Charbit et al., 2008) show that on the millennial time scale, the GIS can melt completely if temperatures stay above a certain threshold, which is probably just a few degrees above present-day temperatures (Gregory et al., 2004). In view of the extremely long lifetime of CO_2 in the atmosphere (Archer, 2005), such a possibility is likely if a considerable portion of the remaining conventional fossil fuels will be used.

For the 21st century, a number of coupled general circulation model (GCM) runs for several emission scenarios are available and can be used to force ice sheet models. The use of high-resolution, regional models driven by GCMs could additionally improve the representation of climate change over Greenland. However, for longer time scales, coupled GCMs are not only computationally expensive, but gradual changes in the topography and ice sheet extent should also be taken into account. This requires bi-directional coupling between climate and ice sheet models, which makes these models even more expensive. So far, only a few experiments of this sort have been performed, using rather coarse resolution climate models (e.g., Ridley et al., 2005; Mikolajewicz et al., 2007; Vizcaíno et al., 2008).

Most studies of the short- and long-term response of the GIS to global warming use a rather simple approach, in which a simulated temperature anomaly field or a constant temperature offset is added to the modern climatological temperatures and a simple correction for elevation change is employed (e.g., Greve, 2000; Huybrechts et al., 2004; Parizek and Alley, 2004; Gregory and Huybrechts, 2006). While such an approach is justified for short-term predictions, it becomes less applicable on longer time scales, when the GIS can change dramatically. Changes in ice sheet extent and elevation will lead to pronounced changes in temperature and precipitation patterns. In particular, the reduction in surface albedo due to a retreat of the ice sheet would cause a large temperature change that would not be captured by a simple elevation correction. These changes would also affect the spatial distribution and seasonality of precipitation, as well as the relative amount of precipitation falling as snow.

The representation of accumulation over the ice sheet using the conventional approach suffers further limitations, in that (1) estimates of the present day annual accumulation rate are derived from a rather sparse observational network (Bales et al., 2009), and (2) real precipitation over Greenland exhibits significant seasonality. Since most precipitation over the GIS currently occurs in the form of snow, the use of an annual accumulation field does not pose a serious problem for modeling the surface mass balance. However, under a much warmer climate, the fraction of liquid precipitation over the GIS is expected to increase considerably, which may offset the effect of a general increase in total precipitation. In addition, present day precipitation over the GIS is, to a large extent, topographically controlled. Changes in the elevation (let alone a complete disappearance of the GIS) would have a pronounced effect on the distribution of precipitation over the GIS.

To overcome some of the limitations of the conventional approach, particularly when used for long-term simulations of the GIS, we developed a new approach based on a regional energy and moisture balance model. Though relatively simple compared to regional climate models, our approach accounts for the most essential physical processes. It should therefore be considered as a physically-based downscaling technique, rather than a regional climate model on its own. This approach can be used to determine realistic temperature and precipitation fields over Greenland, given topographic and climatic conditions that are dramatically different from today. Importantly, it is also computationally efficient enough to permit long-term simulations of the response of the GIS to climate change. The model is evaluated here for both present-day and ice-free topographic conditions.

Furthermore, in most previous modeling studies, surface ablation has been simulated using the positive degree day (PDD) method. Besides several applications on a smaller scale (e.g., Braithwaite, 1980), the PDD method has also been utilized to calculate surface ablation in large-scale models of the GIS (e.g., Reeh, 1991; Huybrechts et al., 1991; Calov and Hutter, 1996; Ritz et al., 1997; Janssens and Huybrechts, 2000; Huybrechts et al., 2004). In this method, surface melt is explicitly determined from surface air temperature alone. The effect of insolation on surface melt is accounted for implicitly, via different empirical coefficients for snow and ice. Although the method has been successfully tested against present day empirical data, its applicability to future climate change may be compromised, since the relationship between temperature and insolation will be different under global warming induced by greenhouse gases. Indeed, in this case, the temperature will rise while insolation remains constant.

In contrast to the PDD method, another simplified method for computing surface ablation explicitly includes the effects of both temperature and insolation. It has recently been employed by van den Berg et al. (2008) to simulate ice sheet changes through glacial cycles. Such a parameterization was introduced early on by Pollard (1980), found its application to the simulation of the evolution of ice sheets during the ice ages (Esch and Herterich, 1990; Deblonde and Peltier, 1992; Peltier and Marshall, 1995) and is nowadays becoming more prevalent in ice sheet modeling (e.g., Hebeler et al., 2008). For convenience, we will call it the insolation-temperature melt (ITM) method. ITM requires essentially the same input as the PDD method and it is also computationally efficient, allowing its use for long-term simulations. As it is not known a priori which approach provides more realistic ice sheet forcing, a comparison of both methods could help quantify uncertainties in future predictions related to the choice of the mass balance scheme.

2 Model description

The model used here to compute the surface boundary conditions over the GIS consists of two parts: (1) the regional energy-moisture balance orographic model (REMBO) that computes surface air temperature and precipitation; and (2) the surface interface, which provides surface ice temperature and surface mass balance to the ice sheet model. Both REMBO and the surface interface calculate daily fields, which allow seasonal variations in surface albedo to affect the climate. This provides an important positive feedback, since changes in planetary albedo (via changes in surface albedo) affect the computed temperature and surface mass balance. In turn, changes in topography, simulated by the ice sheet model, affect the simulated climatology via elevation and slope effects (see Sect. 2.1).

The REMBO model is coupled via the surface interface to the ice sheet model SICOPOLIS (Version 2.7, Greve, 1997a). SICOPOLIS is a three-dimensional polythermal ice sheet model, which is based on the shallow-ice approximation. Its main difference to other ice sheet models is the treatment of the temperate basal ice layers, in which the total heat flux and the diffusive water flux are calculated assuming a mixture of water and ice (Greve, 1997b). The cold ice regions are treated similar to other thermomechanical ice sheet models via a temperature/energy balance equation including vertical diffusion, three-dimensional advection and dissipation terms.

While REMBO calculates fields on a lower resolution grid (100 km), surface boundary conditions are computed via the surface interface on the grid of the ice sheet model, which has a higher spatial resolution (20 km). This allows the surface interface to better resolve the rather narrow ablation zone on the margin of the ice sheet. We also performed equilibrium experiments with a spatial resolution of 10 km for the ice sheet model and surface interface and found minimal difference between the results obtained for the two grids. Therefore, all simulations presented hereafter were performed using the 20 km grid. The high resolution topography and surface albedo computed on the 20 km grid are aggregated to the 100 km grid of REMBO and are then used in the computations of surface temperature and precipitation. In turn, surface temperature and precipitation computed by REMBO are interpolated onto the 20 km grid to provide input for computing the surface boundary conditions for the ice sheet model. To compute the surface mass balance, we used the two potential melt models mentioned in the introduction: PDD and ITM. In Sect. 3, we will compare results obtained using these two approaches.

2.1 Regional energy-moisture balance model

The energy balance model follows a familiar form, first employed by Budyko (1969) and Sellers (1969), and reviewed by North (1981), and is still found in most simplified climate models. The equation for the atmospheric moisture budget, similar to that for temperature, was later added to energy balance models to simulate precipitation (e.g., Fanning and Weaver, 1996). Unlike existing energy and moisture-balance models, which are global, the model employed in this study is regional and only applied over Greenland. Compared to conventional approaches used for forcing the long-term simulation of GIS evolution, the REMBO model provides a number of important advantages, because it explicitly accounts for the ice-albedo feedback, the effect of continentality and the orographic effect on precipitation.

REMBO is based on two-dimensional, vertically integrated equations for energy (temperature) and water content in the atmosphere. The two prognostic variables are sea level temperature and specific humidity. The temperature and moisture balance equations are only solved over Greenland. Over the boundary ocean, surface air temperature and relative humidity are prescribed, either from climatology or global climate model results. These governing equations are based on a number of assumptions. First, it is assumed that the lateral exchange of energy and moisture can be described in terms of macroturbulent diffusion, which implies the dominance of synoptic-scale processes over mean horizontal advection. Second, we assume that changes over Greenland do not affect the climate outside it, i.e., we consider only uni-directional interaction. Third, vertical temperature and humidity profiles are assumed to have a universal structure (e.g., Petoukhov et al., 2000). Finally, the heat capacity of the active soil or snow/ice layer is neglected.

The vertically-integrated energy balance for the total atmospheric column is written in terms of the sea-level temperature T_{SL} as

$$c_p \rho_a H_a \frac{\partial T_{SL}}{\partial t} = D_T \nabla^2 T_{SL} + (1-\alpha_p)S - [A + BT] + L_w P_w + L_s P_s - L_s M_i + R(\mathrm{CO_2}), \quad (1)$$

TCD
3, 729–764, 2009
An efficient regional energy-moisture balance model
A. Robinson et al.

where the first term on the right side of the equation represents the horizontal diffusion of the temperature, second – absorbed solar radiation, third – outgoing long-wave radiation, fourth to sixth – latent heat related to condensation of liquid water, snow formation and surface melting of snow/ice, respectively, and the last term – radiative forcing of CO_2 relative to the preindustrial state (set to zero in this study), c_p is the air heat capacity , ρ_a is the air density, H_a is the atmospheric height scale, D_T is the coefficient of horizontal energy diffusion, S is the insolation at the top of the atmosphere, α_p is the planetary albedo, A and B are empirical coefficients in Budyko's parameterization of outgoing long-wave radiation, P_w and P_s are precipitation in liquid and solid form, M_i is the surface melt rate, and L_w and L_s are the latent heats of condensation and snow formation, respectively. The surface temperature, T, is then related to the sea-level temperature by surface elevation z_s, multiplied by the free atmospheric lapse-rate, γ_a,

$$T = T_{SL} - \gamma_a z_s \,. \tag{2}$$

Next, the moisture balance equation is written as

$$\rho_a H_e \frac{\partial Q}{\partial t} = D_Q \nabla^2 Q - P \,, \tag{3}$$

where Q is the surface air specific humidity, H_e is the water vapor scale height, D_Q is the coefficient of horizontal macroturbulent moisture diffusion and P is the total precipitation. To make the model applicable to simulation of different climate states, outside of the modeling domain, we prescribed relative humidity rather than specific humidity, since the former is less sensitive to temperature changes than the latter. Therefore, the boundary value for specific humidity is computed from the formula

$$Q = Q_{\mathrm{sat}}(T) r \,, \tag{4}$$

where r is the relative humidity and $Q_{\mathrm{sat}}(T)$ is the saturation specific humidity, which is described by the Clausius-Clayperon function of air temperature. The total amount

TCD

3, 729–764, 2009

An efficient regional energy-moisture balance model

A. Robinson et al.

of precipitation is computed, following an approach similar to that of Petoukhov et al. (2000) and Calov et al. (2005), as

$$P = \left(1 + k|\nabla z_s|\right)\left(\frac{Q}{\tau}\right) . \quad (5)$$

Here $|\nabla z_s|$ is the module of the gradient of surface elevation, τ is the water turnover time in the atmosphere, and k is an empirical parameter. Note that Eq. (5) is also similar to that used by van den Berg et al. (2008), in that precipitation is strongly dependent on elevation changes.

The amount of snowfall at each point is calculated as a fraction of the total precipitation,

$$P_s = P\,f(T) , \quad (6)$$

where the fraction, f, depends on the surface temperature. Below a minimum temperature, this fraction is 1 (all precipitation falls as snow), and above a maximum temperature, this fraction is 0 (no snow). The fraction follows a sine function from 1 to 0 between the minimum and maximum temperatures, which were set to −11.6°C and 7.4°C, respectively, as these were found to be the limits from fits to empirical data over Greenland (Bales et al., 2009; Calanca et al., 2000).

The diffusion coefficients, D_Q and D_T, in Eqs. (1) and (3), both decrease linearly with latitude ϕ (in degrees), and D_T also increases linearly with surface elevation z_s (in meters):

$$D_Q = (1 - 0.01\varphi) \cdot \kappa_Q , \quad (7)$$

$$D_T = (1 + 0.00125 z_s)(1 - 0.01\varphi) \cdot \kappa_T , \quad (8)$$

where κ_Q and κ_T are the diffusion constants for moisture and temperature, respectively.

Outgoing long-wave radiation is parameterized as a linear function of surface air temperature. The values of parameters A and B were found using values for upward long-wave radiation and surface temperature over Greenland from the European Center for Medium Range Weather Forecasts (ECMWF) Reanalysis 40 (ERA-40) data set (Uppala et al., 2005), shown in Fig. 1a. Monthly climatological data over the entire year were used, and the best fit to these data gave parameter values close to those used by Budyko (1969). These and other important numerical parameters of the model are summarized in Table 1.

Planetary albedo is parameterized as a linear function of surface albedo (Fig. 1b). The fit was found from values of surface and planetary albedo, derived from monthly International Satellite Cloud Climatology Project (ISCCP) radiation data (Schiffer, 1985), and is given by

$$\alpha_p = 0.35 + 0.39\alpha_s \,. \tag{9}$$

Only summer values (April–September) were used to obtain the fit, since at high latitudes, insolation in winter is insignificant, thus the winter albedo is not relevant. Surface albedo α_s is calculated as a function of ground albedo (ice or bare soil) and the snow thickness following Bintanja (2002) and van den Berg et al. (2008),

$$\alpha_s = \min\left(\alpha_g + \frac{d}{d_{\text{crit}}}\left(\alpha_{s,\max} - \alpha_g\right), \alpha_{s,\max}\right) \,. \tag{10}$$

The maximum snow albedo, $\alpha_{s,\max}$, has a value of either 0.8 or 0.6, representing either a dry-snow or wet-snow covered surface, respectively. The value is chosen based on whether any melting has occurred at that location on that day. The ground albedo, α_g, has a value of 0.4 for ice and 0.2 for ice-free land. If no snow is present, the surface albedo equals the ground albedo. Comparison with the ISCCP satellite data for radiation at the surface shows that this parameterization provides a quite realistic range of values of surface albedo for Greenland. A more detailed comparison is limited, since the data are only available at a spatial resolution of 2.5°.

To prescribe boundary conditions for temperature and humidity, we used ERA-40 data (Uppala et al., 2005), since the ECMWF reanalysis data sets have been shown to be quite realistic in representing important climate variables for the Greenland region (Hanna and Valdes, 2001; Hanna et al., 2005). Monthly climatological fields (averaged from 1958 to 2001) of temperature and relative humidity from the 2.5° ERA-40 grid were bi-linearly interpolated in space to the Cartesian 100 km grid used in REMBO. In addition, temperature fields were corrected for elevation differences (Hanna et al., 2005) between ERA-40 and REMBO using, for simplicity, the free atmospheric lapse rate γ_a=0.0065 K/m.

The equations for temperature and moisture (Eqs. 1 and 3) are solved using an alternating-direction implicit discretization scheme, which allows a larger time step than a standard explicit scheme. Still, for numerical stability reasons, the time step used to solve the energy balance equations is quite small, on the order of 1/10 of a day and, therefore, the REMBO model is much more computationally demanding than the ice sheet model. This does not present a problem for short-term (decadal to centennial time scale) simulations, but for millennial and longer simulations, asynchronous coupling between REMBO, the surface interface and the ice sheet model was used. In the equilibrium runs described below, the surface mass balance interface was only called for every ten ice sheet model years and REMBO was called for every one hundred ice sheet model years. This calling frequency would affect the transient behavior of the GIS somewhat, but not the simulated equilibrium state reached after several thousand years.

2.2 Surface mass balance

Annual mean surface boundary conditions for the ice sheet model are provided by a simple surface interface. Surface ice temperature is determined at each time step as $T_i = \min(T, 0)$, and then averaged over one year. Annual surface mass balance is computed through equations of snow (h_s) and ice (h_i) thickness in water equivalent, calculated for each day over the year:

$$\frac{dh_s}{dt} = P_s - M_s(1 - r_f), \qquad h_s \in (0, h_{s,\max}), \tag{11}$$

$$\frac{dh_i}{dt} = \begin{cases} M_s r_f\,, & h_s > 0 \\ \min(P_s - M_s, 0)\,, & h_s = 0 \end{cases}\,, \tag{12}$$

where M_s is the potential surface melt rate and r_f is the refreezing fraction. Snow cover thickness is not allowed to exceed a maximum height of $h_{s,\max}$=5 m (in water equivalent). At each time step, any excess of snow thickness above this limit is added to the ice thickness computed by Eq. (12), and snow thickness is reset to 5 m. The refreezing fraction is equal to zero in the absence of snow, while for h_s>0, it is defined following Janssens and Huybrechts (2000) as

$$r_f = r_{\max} f(T)\,, \tag{13}$$

where $f(T)$ is the fraction of snow of the total precipitation, and $r_{\max}$ is equivalent to the "PMAX" factor originally described by Reeh (1991). The annual mean surface mass balance of the ice sheet is then computed at the end of each year as the difference between the final and initial thickness of the ice.

The daily potential surface melt rate used in the calculation of surface mass balance is either obtained from the PDD or ITM method, both of which are described below.

2.2.1 Positive degree day method

The PDD method is the conventional approach used to determine the melt potential of a given year, using calculated positive degree days from a seasonal cycle of temperature. It has been described by several others and is consistently used for ice sheet model surface forcing (e.g., Ritz et al., 1997; Cuffey and Marshall, 2000; Huybrechts et al., 2004; Charbit et al., 2007).

To account for inter- and intra-annual variability, an "effective" daily temperature, T_{eff}, is calculated from the daily temperature, T_m, as

$$T_{\mathrm{eff}} = \frac{1}{\sigma\sqrt{2\pi}} \int_0^{\infty} T \exp\left(\frac{-(T - T_m)^2}{2\sigma^2}\right) dT\,. \tag{14}$$

The value of standard deviation σ was set to 5°C, as in many previous studies, and T_{eff} was numerically calculated according to the method described by Calov and Greve (2005). In the conventional approach, the annual positive degree days (PDDs) are computed as the sum of the effective temperature over the year. In our case, since the model resolves the seasonal cycle, the effective temperature is used to compute daily potential melt rate in much the same way, as

$$M_s = b\,T_{\text{eff}}\,, \tag{15}$$

where the empirical coefficient b_s=0.003 mie/(day K) for snow and b_i=0.008 mie/(day K) for ice (and mie=meters ice equivalent).

2.2.2 Insolation-temperature melt method

The ITM method is based on the work of Pellicciotti et al. (2005) and van den Berg et al. (2008). In this method, the potential surface melt rate is determined from surface air temperature and absorbed insolation:

$$M_s = \frac{1}{\rho_w L_m}[\tau_a(1-\alpha_s)S + c + \lambda T]\,, \tag{16}$$

where τ_a is the transmissivity of the atmosphere (i.e., the ratio between downward shortwave radiation at the land surface and at the top of the atmosphere), α_s is the surface albedo, S is the insolation at the top of the atmosphere and λ and c are empirical parameters. Unlike the PDD method, this method explicitly accounts for shortwave radiation, and the difference between snow and ice is expressed in Eq. (16) via different surface albedo values.

Based on the summer (April–September) ISCCP radiation data, the transmissivity over Greenland was found to have a slight elevation dependence, with values ranging from about 0.4 to 0.7 (Fig. 1c). The linear fit was provided by

$$\tau_a = 0.46 + 0.00006\,z_s\,, \tag{17}$$

where z_s is the surface elevation in meters. The winter data were again not used for the fit, because such low values of incoming radiation increase the data spread, making any trend indiscernible. It should be noted that, at lower elevations, where the shortwave radiation term in the melt equation is more significant, the value of transmissivity is similar to the value of 0.5 used by van den Berg et al. (2008).

The parameter λ was set to 0.3, equivalent to that used by van den Berg et al. (2008), while c was used as a free parameter to best reproduce the present-day GIS, here found to have a value of $-50\,\mathrm{W/m^2}$.

3 Modeling results

In order to evaluate the performance of REMBO and the melt models, we first performed simulations with the fixed, present-day topography of Greenland and modern climatological lateral boundary conditions. These results were compared with observations and a conventional parameterization of climate forcing used in the European Ice Sheet Modeling Initiative (EISMINT) intercomparison project and many recent publications (Huybrechts et al., 1997). Melt and surface mass balance were also diagnosed from these experiments and compared with existing empirical and modeling estimates. REMBO was then coupled with the ice sheet model SICOPOLIS to simulate the equilibrium ice sheet. The equilibrium simulations were performed using both the PDD and ITM surface melt approaches.

3.1 Simulations of climatology and mass balance with fixed topography

For diagnostic simulations of the present-day climatology and surface mass balance of the GIS, we used the 5 km resolution gridded topography from Bamber et al. (2001), aggregated to the resolution of the ice sheet model (20 km). Temperature and accumulation fields obtained from REMBO for the present-day Greenland topography have been compared to best estimates from observational data sets (correcting for elevation differences via the free atmospheric lapse rate). Several coastal observations were obtained from Technical Report 00-18 of the Danish Meteorological Institute (Cappelen, 2001), which provides long-term means of various climatic variables taken from automatic weather stations. Other observations were obtained from the GC-Net program for locations on the ice sheet itself (Steffen et al., 1996). Although the earliest GC-Net observations only began in 1995, they are the best resource available currently. The combination of these datasets provided monthly observations from 52 station locations.

Temperatures from REMBO agree well with the observations, with an annual mean residual of $-0.23\pm2.57^{\circ}$C. Temperatures obtained from the EISMINT parameterization (corrected for elevation differences via the parameterization's lapse rates) also match observational data almost perfectly in the annual mean, with a residual of $0.05\pm3.58^{\circ}$C. However, this agreement in annual mean masks some systematic seasonal biases, which are not present in REMBO simulations (Fig. 2a). REMBO temperatures around the Greenland coast are determined by the boundary ERA-40 reanalysis temperatures over the ocean. Since the analysis by Hanna et al. (2005) revealed very good agreement of ERA-40 temperatures with station data, the consistency of the REMBO temperatures with empirical data around the coast is not surprising. The EISMINT temperatures are directly based on coastal temperature data, but nonetheless show a slight warm bias at low elevations, as exemplified by the DMI station at Daneborg (id 4330), shown in Fig. 2b.

At higher elevations on the ice sheet, where REMBO-simulated temperatures have more freedom to evolve away from the boundary conditions, the observed seasonal temperature variability is reproduced, except for a small cold bias. An example GC-NET high elevation station at Summit (id 06) is given in Fig. 2b. The EISMINT parameterization matches summer temperatures reasonably well, but winter temperatures are usually underestimated.

The actual annual and summer temperatures predicted using REMBO can be seen in Fig. 3a and b, respectively. The differences between these temperatures and those obtained via the EISMINT parameterization are shown in Fig. 3c and d. Both the annual and summer temperatures are quite comparable, although there are notable differences in the annual mean temperature at high elevation. This is because the EISMINT parameterization generally underestimates the winter temperature for high elevations. This difference has little practical effect on ice sheet modeling for present day, given that temperatures at higher elevation remain well below freezing throughout the year. The summer temperatures compare especially well around the coast and margin of the ice sheet, where temperature is most important for diagnosing melt.

Figure 4 shows annual accumulation and total precipitation patterns simulated by REMBO, as well as the most recent estimates obtained from station data and several ice core samples, compiled by Bales et al. (2009). The simulated fields agree reasonably well with observations, despite some local discrepancies. Particularly, there is low accumulation in the north and on the highly elevated central part of the GIS, while high accumulation values can be found along the Southeast coast. In REMBO, the gradient of elevation mainly determines how much precipitation will occur, implying that it is a result of orographic uplifting. Notably, however, REMBO produces too much snow on the southwest coast and the southern tip of Greenland – an indication that local circulation may play a role that is not accounted for here. The annual accumulation total for the GIS simulated by REMBO is ca. 530 Gt/a, which is within an acceptable range of the best estimate of ca. 560 Gt/a from Bales et al. (2009).

Given the accumulation and temperature fields, it is then possible to diagnose the surface mass balance of the ice sheet (Fig. 5). Using the fixed, present-day topography, REMBO was coupled with each melt model. The PDD approach results in an almost quadratic reduction of melt with altitude, so most melt occurs at lower elevations. Conversely, the ITM approach produces melt that linearly decreases with altitude, allowing for more intense melt at higher elevations. Using both approaches, the overall area of melt predicted is fairly consistent – although more melt area is determined in the north using the ITM approach. Mean annual diagnosed ablation is found to be ca. 450 Gt when calculated with both the PDD and the ITM approaches, which is significantly higher than the empirical estimate of ca. 300 Gt (IPCC TAR, 2001). Total annual ablation decreases once the ice sheet model is allowed to equilibrate (see Table 2).

Simulations were also performed with a fixed topography of ice-free Greenland with corresponding uplifted bedrock (i.e., equilibrium bedrock after isostatic rebound). This test provides insight into the sensitivity of the REMBO climate to the presence of the ice sheet and can be compared with similar GCM simulations. It is also noteworthy to compare REMBO results with the EISMINT parameterization, which clearly demonstrates the advantages of a more physically-based approach.

Figure 6a and b show the difference in the mean summer (June-July-August) temperature between the ice-free and present-day Greenland simulations, obtained with the EISMINT parameterization and with REMBO, respectively. Both modeling approaches produce qualitatively similar warming patterns associated with the lowering of elevation over currently ice-covered Greenland. However, there are significant quantitative differences. REMBO shows a surface air temperature increase of more than 15°C in summer and only 10°C in winter over the central part of Greenland. These numbers agree favorably with the results of simulations performed with a GCM for ice-free Greenland (Toniazzo et al., 2004). At the same time, the EISMINT approach produces an inverse situation: 10°C summer and 15°C winter warming. As a result, REMBO shows that the magnitude of seasonal temperature variation over central Greenland increases by more than 8°C for ice free conditions (Fig. 6c), while the EISMINT parameterization shows a decrease of 6°C (Fig. 6d). The increase of seasonality and stronger summer warming in the REMBO model can be attributed to the additional warming caused by a lower albedo for ice free conditions during summer, while winter albedo remains practically unaffected by the removal of the ice sheet. The result is stronger warming in the summer and, therefore, an increase in seasonality. The opposite effect produced by the EISMINT parameterization is explained by the higher lapse rate used in winter. As a result, the decrease in elevation leads to a reduction of the temperature difference between summer and winter and a decrease in seasonality. Since the REMBO model explicitly accounts for both albedo and continentality effects, there is good reason to expect that REMBO is more appropriate than the EISMINT parameterization for modeling climate conditions considerably different from present day.

3.2 Coupled simulations of equilibrium state

For the next step of model validation, we performed equilibrium simulations of the GIS with constant (present-day) climatological conditions at the lateral boundaries of the model domain. The REMBO model and the surface interface were coupled bi-directionally and asynchronously with SICOPOLIS, which was run for 150 000 years, ensuring all relevant characteristics reached equilibrium state. As an initial condition, we used present-day data for the GIS elevation and bedrock (Bamber el al., 2001), and the ice temperature was set to 0°C. The geothermal heat flux was constant and set to 60 mW/m^2. Since the longest time scale of GIS response is comparable with orbital time scales, an assumption about GIS equilibrium forced only by present-day conditions is not very accurate and, instead, a simulation over several glacial cycles would be a more appropriate procedure. However, because here we are primarily interested in understanding the sensitivity of the simulated GIS to the different methods for determining the surface boundary conditions, we prefer the simpler approach of using constant climatological forcing.

Given the good agreement between the REMBO and EISMINT approaches in simulating temperature and accumulation fields, it is not surprising that using either climatology combined with the PDD melt scheme produces quite similar results (shown in Fig. 7a and b). In both cases, the simulated equilibrium ice sheet covers almost the entire area of Greenland, which also occurs in other GIS simulations using similar approaches (Letréguilly et al., 1991; Calov and Hutter, 1996; Ritz et al., 1997; Greve, 2005). The main difference appears in the southwest, where using the REMBO climatology results in more extended ice coverage. However, this is mainly due to the overestimation of accumulation there by REMBO, as discussed in Sect. 3.1.

In contrast, combining REMBO with the ITM method produces an equilibrium ice sheet that, while still somewhat too large (Fig. 7c), agrees better with empirical data (Fig. 7d). Simulated ice sheet extent in the northern part of Greenland is limited by the more intense melt produced by the ITM method, and there is a better fit in the southwest. In our simulations, the area and volume of the GIS, as well as the total ablation, are overestimated when compared to the empirical estimates (see Table 2 for a summary of the equilibrium volume and surface mass balance components). In other words, it was not possible to simulate an ice sheet, which has both the right geometry and the right mass balance components. This may be related, not so much to the deficiencies of the model used for simulation of the surface mass balance, but rather to an intrinsic problem of ice sheet models based on the shallow ice approximation. Since such models do not properly incorporate fast ice transport by ice streams, they require too much contact between the ice sheet and the ocean to produce a considerable amount of ice calving. In reality, the areas where the GIS is in direct contact with the ocean are rather small and yet, ice calving constitutes roughly half of the total ice loss from the GIS.

It has been proposed that under modern climate conditions, the GIS may have two different equilibrium states – ice-covered Greenland (similar to present day) and an ice-free state (Crowley and Baum, 1995; Toniazzo et al., 2004; Ridley et al., 2009). To test this hypothesis, we performed two additional equilibrium runs which differ from that described above, only in that the *initial* topography of Greenland was specified as ice-free with uplifted bedrock. Experiments were performed with the two different melt schemes (PDD and ITM). Although initially both schemes predict similar small areas of positive mass balance over Greenland, concentrated in the elevated mountain regions (Fig. 8), the equilibrium states attained after 150 000 model years using each melt model were fundamentally different (Fig. 9). When using PDD forcing, the equilibrium GIS is identical to that obtained when the present-day GIS is used for the initial topography. Therefore, in this case, only one equilibrium state exists under present-day climate forcing (note that this does not rule out the possibility of multi-stability for other climate states). However, using the ITM approach, only a partially-glaciated Greenland was obtained with two ice caps located over the elevated southern and eastern parts of Greenland. The total volume of the GIS in this case is only 16% of the fully glaciated

Greenland equilibrium state. Therefore, our simulations do not provide an unambiguous answer on the bistability of the GIS under modern climate conditions, but they do indicate that there is likely a strong dependence of results on the chosen melt scheme.

4 Conclusions

A regional energy-moisture balance model (REMBO) has been developed, which simulates temperature and precipitation over Greenland. The model is simple and very computationally efficient. Furthermore, it is physically-based and includes an explicit representation of seasonal changes in albedo – attributes that are crucial for simulation of climate conditions considerably different from present day.

Simulated temperature and accumulation fields agree well with both observational data and the EISMINT temperature parameterization. However, for ice-free conditions, REMBO and the EISMINT parameterization predict rather different changes. REMBO simulates a large summer warming and enhanced magnitude of seasonal temperature changes, while the EISMINT parameterization shows decreased seasonality. In this respect, the results from REMBO are more consistent with GCM experiments.

Two different melt schemes were coupled to REMBO: the conventional PDD method and the ITM method, with the latter explicitly accounting for the effects of temperature and insolation on snow and ice melt. Within the uncertainties of parameters, both methods produce similar total ablation rates for present-day conditions, but they differ in regional details.

Equilibrium simulations of the present-day GIS with REMBO coupled to the three-dimensional, polythermal ice sheet model SICOPOLIS demonstrate that both melt models allow us to simulate a reasonably realistic GIS. However for both methods, the simulated volume and spatial extent of the GIS are slightly overestimated. Nonetheless, the ITM method looks preferable for long-term and paleo simulations, due to its explicit physical link to short-wave radiation.

However, when initializing equilibrium runs with ice-free conditions, the two different

TCD
3, 729–764, 2009

approaches to calculating surface mass balance produce fundamentally different results. Using the PDD approach, the simulated equilibrium ice sheet fully regrows to the present-day configuration, while using the ITM approach produces only two relatively small ice caps covering the high latitude areas of southern Greenland. These results indicate that simulations of the GIS can be rather sensitive to the choice of melt scheme, and leave open the question of GIS bi-stability for the present day.

Acknowledgements. We would like to thank R. Greve for providing us with the ice sheet model SICOPOLIS. A. Robinson is funded by the European Commission's Marie Curie 6th Framework Programme, and is a part of the Research Training Network, Network for Ice and Climate Interactions (NICE), and R. Calov is funded by the Deutsche Forschungsgemeinschaft RA 977/6-1. ERA-40 Reanalysis data was provided by the ECMWF and obtained from their website. GC-NET data was provided by K. Steffen via the GC-NET portal. Radiation data was obtained from the International Satellite Cloud Climate Project (ISCCP) website.

References

Abdalati, W. and Steffen, K.: Greenland ice sheet melt extent: 1979–1999, J. Geophys. Res., 106(D24), 33, 983–988, 2001.

Archer, D.: The fate of fossil fuel CO_2 in geologic time, J. Geophys. Res., 110, C09S05, doi:10.1029/2004JC002625, 2005.

Bales, R. C., Guo, Q., Shen, D., McConnell, J. R., Du, G., Burkhart, J. F., Spikes, V. B., Hanna, E., and John Cappelen, J.: Annual accumulation for Greenland updated using ice-core data developed during 2000–2006 and analysis of daily coastal meteorological data, J. Geophys. Res., 114, D06116, doi:10.1029/2008JD011208, 2009.

Bamber, J. L., Ekholm, S., and Krabill, W. B.: A new, high-resolution digital elevation model of Greenland fully validated with airborne laser altimeter data, J. Geophys. Res., 106(B4), 6733–6745, 2001.

Bintanja, R., van de Wal, R. S. W., and Oerlemans, J.: Global ice volume variations through the last glacial cycle simulated by a 3-D ice-dynamical model, Quatern. Int., 95–96, 11–23, 2002.

Box, J. E., Bromwich, D. H., Veenhuis, B. A., Bai, L. S., Stroeve, J. C., Rogers, J. C., Steffen, K., Haran, T., and Wang, S. H.: Greenland ice sheet surface mass balance variability (1988–2004) from calibrated polar MM5 output, J. Climate, 19, 2783–2800, 2006.

Braithwaite, R. J.: Regional Modelling of ablation in West Greenland, Gronlands Geologiske Undersogelse, Copenhagen, nr. 98, 1980.

Budyko, M. I.: The effect of solar radiation variations on the climate of the earth, Tellus, 21, 611–619, 1969.

Calanca, P., Gilgen, H., Ekholm, S., and Ohmura, A.: Gridded temperature and accumulation distributions for Greenland for use in cryospheric models, Ann. Glaciol., 31, 118–120, 2000.

Calov, R. and Hutter, K.: The thermomechanical response of the Greenland ice sheet to various climate scenarios, Clim. Dynam., 12, 243–260, 1996.

Calov, R. and Greve, R.: A semi-analytical solution for the positive degree-day model with stochastic temperature variations, J. Glaciol., 51, 173–175, 2005.

Calov, R., Ganopolski, A., Claussen, M., Petoukhov, V., and Greve, R.: Transient simulation of the last glacial inception with an atmosphere-ocean-vegetation-ice sheet, Part I: Glacial inception as a bifurcation of the climate system, Clim. Dynam., 24, 545–561, 2005.

Cappelen, J., Jørgensen, B. V., Laursen, E. V., Stannius, L. S., and Thomsen, R. S.: The observed climate of Greenland, 1958–1999 – with Climatological Standard Normals, 1961–1990, Danish Meteorological Institute, Copenhagen, 2001.

Charbit, S., Paillard, D., and Ramstein, G.: Amount of CO_2 emissions irreversibly leading to the total melting of Greenland, Geophys. Res. Lett., 35, L12503, doi:10.1029/2008GL033472, 2008.

Church, J. A., Gregory, J. M., Huybrechts, P., et al.: Changes in Sea Level, in: Climate Change 2001: The Scientific Basis: Contribution of Working Group I to the Third Assessment Report of the Intergovernmental Panel on Climate, edited by: Houghton, J. T., Ding, Y., Griggs, D. J., Noguer, M., Van der Linden, P. J., Dai, X., Maskell, K., and Johnson, C. A., Cambridge, Cambridge University Press, 641–693, 2001.

Crowley, T. J. and Baum, S. K.: Is the Greenland ice sheet bistable? Paleoceanography, 10, 357–363, 1995.

Cuffey, K. M. and Marshall, S. J.: Substantial contribution to sea-level rise during the last interglacial from the Greenland ice sheet, Nature, 404, 591–594, 2000.

Deblonde, G., Peltier, W. R., and Hyde, W. T.: Simulations of continental ice sheet growth over the last glacial-interglacial cycle: Experiments with a one level seasonal energy balance

model including seasonal ice albedo feedback, Global Planet. Change, 6, 37–55, 1992.
Esch, M. B. and Herterich, K.: A two-dimensional coupled atmosphere-ice-sheet-continent model designed for paleoclimatic simulations, Ann. Glaciol., 14, 55–57, 1990.
Fanning, A. F. and Weaver, A. J.: An atmospheric energy-moisture balance model: Climatology, interpentadal climate change, and coupling to an ocean general circulation model, J. Geophys. Res., 101(D10), 15111–15128, 1996.
Gregory, J. M and Huybrechts, P: Ice-sheet contributions to future sea-level change, Philos. T. R. Soc. Lond. A, 364, 1709–1731, 2006.
Gregory, J. M., Huybrechts, P., and Raper, S. C. B.: Threatened loss of the Greenland ice-sheet, Nature, 428, p. 616, doi:10.1038/428616a, 2004.
Greve, R.: Relation of measured basal temperatures and the spatial distribution of the geothermal heat flux for the Greenland ice sheet, Ann. Glaciol., 42, 424–432, 2005.
Greve, R.: On the response of the Greenland ice sheet to greenhouse climate change, Climatic Change, 46, 289–303, 2000.
Greve., R.: Application of a polythermal three-dimensional ice sheet model to the Greenland ice sheet: Response to steady-state and transient climate scenarios, J. Climate, 10(5), 901–918, 1997a.
Greve., R.: A continuum-mechanical formulation for shallow polythermal ice sheets, Philos. T. R. Soc. Lond., 355, 1726, 921–974, 1997b.
Hanna, E., Huybrechts, P., Janssens, I., Cappelen, J., Steffen, K., and Stephens, A.: Runoff and mass balance of the Greenland ice sheet: 1958–2003, J. Geophys. Res., 110, D13108, doi:10.1029/2004JD005641, 2005.
Hanna, E. and Valdes, P.: Validation of ECMWF (Re)analysis surface climatedata, 1978–1998, for Greenland and implications for mass balance modeling of the ice sheet, Int. J. Climatol., 21, 171–195, 2001.
Hebeler, F., Purves, R. S., and Jamieson, S. S. R.: The impact of parametric uncertainty and topographic error in ice sheet modeling, J. Glaciol., 54, 899–919, 2008.
Huybrechts, P.: Report of the Third EISMINT Workshop on Model Intercomparison, European Science Foundation, Switzerland, 1997.
Huybrechts, P. and de Wolde, J.: The dynamic response of the Greenland and Antarctic ice sheets to multiple-century climatic warming, J. Climate, 12, 2169–2188, 1999.
Huybrechts, P., Gregory, J., Janssens, I., and Wild, M: Modelling Antarctic and Greenland volume changes during the 20th and 21st centuries forced by GCM time slice integrations,

Global Planet. Change, 42, 83–105, 2004.
Huybrechts, P., Letréguilly, A., and Reeh, N.: The Greenland ice sheet and Greenhouse warming, Palaeogeogr. Palaeocl., 89, 399–412, 1991.
International Satellite Cloud Climatology Project: http://isccp.giss.nasa.gov/projects/browse_fc.html, access: 26 July 2009.
Janssens, I. and Huybrechts, P.: The treatment of meltwater retention in mass-balance parameterizations of the Greenland ice sheet, Ann. Glaciol., 31, 133–140, 2000.
Letréguilly, A., Huybrechts, P., and Reeh, N.: Steady-state characteristics of the Greenland ice sheet under different climates, J. Glaciol., 37, 149–157, 1991.
Mikolajewicz, U., Vizcaíno, M., Jungclaus, J., and Schurgers, G.: Effect of ice sheet interactions in anthropogenic climate change simulations, Geophys. Res. Lett., 34, L18706, doi:10.1029/2007GL031173, 2007.
North, G. R., Cahalan, R. F., and Coakley, J. A.: Energy balance climate models, Rev. Geophys. Space Phys., 19, 91–121, 1981.
Parizek, B. R. and Alley, R. B. R.: Implications of increased Greenland surface melt under global-warming scenarios: Ice-sheet simulations, Quarternary Sci. Rev., 23, 1013–1027, 2004.
Pellicciotti, F., Brock, B., Strasser, U., Burlando, P., Funk, M., and Corripio, J.: An enhanced temperature-index glacier melt model including the shortwave radiation balance: Development and testing for Haut Glacier d'Arolla, Switzerland, J. Glaciol., 51(175), 573–587, 2005.
Peltier, W. R. and Marshall, S.: Coupled energy-balance ice-sheet model simulations of the glacial cycle – a possible connection between terminations and terrigenous dust, J. Geophys. Res., 100, 14269–14289, 1995.
Petoukhov, V., Ganopolski, A., Brovkin, V., Claussen, M., Eliseev, A., Kubatzki, C., and Rahmstorf, S.: CLIMBER-2: A climate system model of intermediate complexity, Part I: Model description and performance for present climate, Clim. Dynam., 16(1), 1–17, 2000.
Pollard, D.: A simple parameterization for ice sheet ablation rate, Tellus, 32, 384–388, 1980.
Reeh, N.: Parameterization of melt rate and surface temperature on the Greenland ice sheet, Polarforschung, 59, 113–128, 1991.
Ridley, J. K., Huybrechts, P., Gregory, J. M., and Lowe, J. A.: Elimination of the Greenland ice sheet in a high CO_2 climate, J. Climate, 18, 3409–3427, 2005.
Ridley, J. K., Gregory, J. M., Huybrechts, P., and Lowe, J. A.: Threshold for irreversible decline of the Greenland ice sheet, Clim. Dynam., doi:10.1007/s00382-009-0646-0, in press, 2009.

Rignot, E., Box, J. E., Burgess, E., and Hanna, E.: Mass balance of the Greenland ice sheet from 1958 to 2007, Geophys. Res. Lett., 35, L20502, doi:10.1029/2008GL035417, 2008.
Rignot, E. and Kanagaratnam, O.: Changes in the velocity structure of the Greenland ice sheet, Science, 311, 986–990, 2006.
Ritz, C., Fabré, A., and Letréguilly, A.: Sensitivity of a Greenland ice sheet model to ice flow and ablation parameters: Consequences for the evolution through the last climatic cycle, Clim. Dynam., 13, 11–24, 1997.
Sellers, W. P.: A global climate model based on the energy balance of the Earth-atmosphere system, J. Appl. Meteorol., 8, 392–400, 1969.
Schiffer, R. A. and Rossow, W. B.: ISCCP global radiance data set: A new resource for climate research, B. Am. Meteorol. Soc., 66, 1498–1505, 1985.
Steffen, K., Box, J. E., and Abdalati, W.: Greenland Climate Network: GC-Net, in: CRREL 96-27 Special Report on Glaciers, Ice Sheets and Volcanoes, trib. to M. Meier, edited by: Colbeck, S. C., USACE Cold Regions Research and Engineering Laboratory, New Hampshire, 98–103, 1996.
Toniazzo, T., Gregory, J., and Huybrechts, P.: Climatic impact of a Greenland deglaciation and its possible irreversibility, J. Climate, 17, 21–33, 2004.
Uppala, S. M., Kellberg, P. W., Simmons, A. J., et al.: The ERA-40 re-analysis, Q. J. Roy. Meteor. Soc., 131(612), 2961–3012, 2005.
van den Berg, J., van de Wal, R. S., and Oerleman, J.: A mass balance model for the Eurasian ice sheet for the last 120 000 years, Global Planet. Change, 61, 194–208, 2008.
Vizcaíno, M., Mikolajewicz, U., Gröger, M., Maier-Reimer, E., Schurgers, G., and Winguth, A.: Long-term ice sheet-climate interactions under anthropogenic greenhouse forcing simulated with a complex earth-system model, Clim. Dynam., 31, 665–690, 2008.
Zwally, H. J., Abdalati, W., Herring, T., Larson, K., Saba, J., and Steffen, K.: Surface melt-induced acceleration of Greenland ice-sheet flow, Science, 297, 218–222, 2002.

Table 1. Selected parameters used in REMBO and the two melt models, PDD and ITM.

Parameter	Units	Best value	Description
REMBO parameters			
κ_T	W/K	2.8e12	Temperature diffusion constant
c_p	J/(K kg)	1000	Air heat capacity
B	$W/(K\,m^2)$	1.97	Long-wave radiation parameter
A	W/m^2	222.3	Long-wave radiation parameter
γ_a	K/m	0.0065	Free atmospheric lapse rate
S	W/m^2	1365	Solar constant
κ_Q	kg/s	8.4e5	Moisture diffusion constant
k	–	50	Precipitation parameter
τ	days	5	Water turnover time
H_a	m	8600	Atmosphere height scale
H_e	m	2000	Water vapor height scale
PDD parameters			
σ	K	5	Standard deviation of temperature normal distribution
b_s	mie/(day K)	0.003	Degree-day factor for snow
b_i	mie/(day K)	0.008	Degree-day factor for ice
ITM parameters			
c	W/m^2	–50	Short-wave radiation and sensible heat flux constant
λ	–	0.3	Long-wave radiation coefficient
Refreezing parameter			
r_{max}	–	0.6	Maximum refreezing fraction

TCD

3, 729–764, 2009

Title Page
Abstract
Introduction
Conclusions
References
Tables
Figures
Back
Close
Full Screen / Esc
Printer-friendly Version
Interactive Discussion

TCD

3, 729–764, 2009

An efficient regional energy-moisture balance model

A. Robinson et al.

Table 2. Equilibrium simulated ice volume and partition of mass balance components for the different melt approaches, compared with best estimates from observations.

	EISMINT, PDD	REMBO, PDD	REMBO, ITM	Observations
Volume (1×10^6 km^3)	3.11	3.26	3.08	2.91[a]
Accumulation (Gt/a)	585	605	576	560[b]
Abalation (Gt/a)	424	435	427	297[c]
Calving (Gt/a)	161	170	149	225[c]

[a] Bamber et al. (2001)
[b] Bales et al. (2009)
[c] IPCC, TAR (2001)

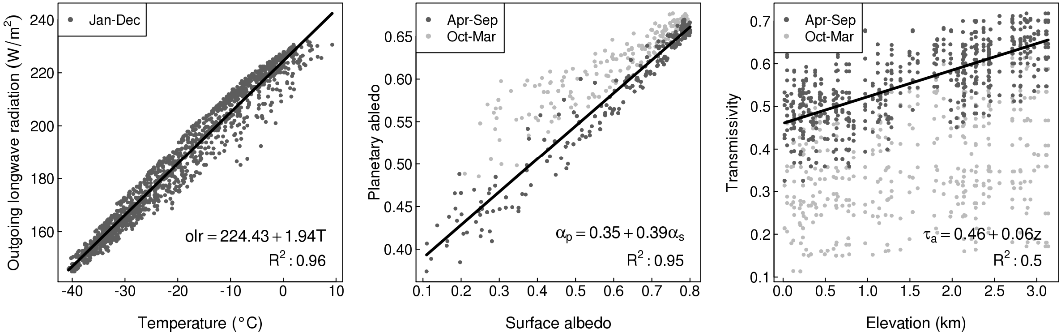

Fig. 1. (a) Monthly ERA-40 data of outgoing long-wave radiative flux versus temperature, shown with a linear fit to all data. Monthly ISCCP data, April–September (dark points) and October–March (light points), of (b) planetary albedo versus surface albedo with a linear fit to the months April–September, and (c) transmissivity versus elevation with a linear fit to the months April–September. All points are from data over Greenland.

TCD

3, 729–764, 2009

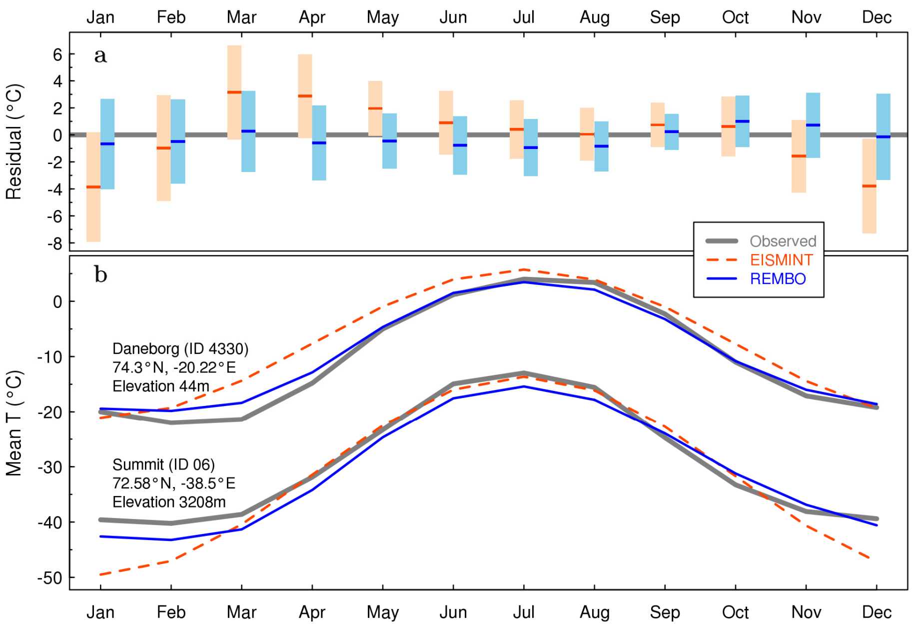

Fig. 2. (a) Average and standard deviation of monthly residuals of REMBO (blue) and EISMINT (red) temperatures compared to station data at 52 locations. **(b)** Monthly temperatures from REMBO (solid blue line) and the EISMINT temperature parameterization (dashed red line), orographically-corrected and compared with DMI station data (thick grey line) for one high- and one low-elevation station on Greenland.

TCD

3, 729–764, 2009

Title Page
Abstract
Introduction
Conclusions
References
Tables
Figures
◀◀
▶▶
◀
▶
Back
Close
Full Screen / Esc
Printer-friendly Version
Interactive Discussion

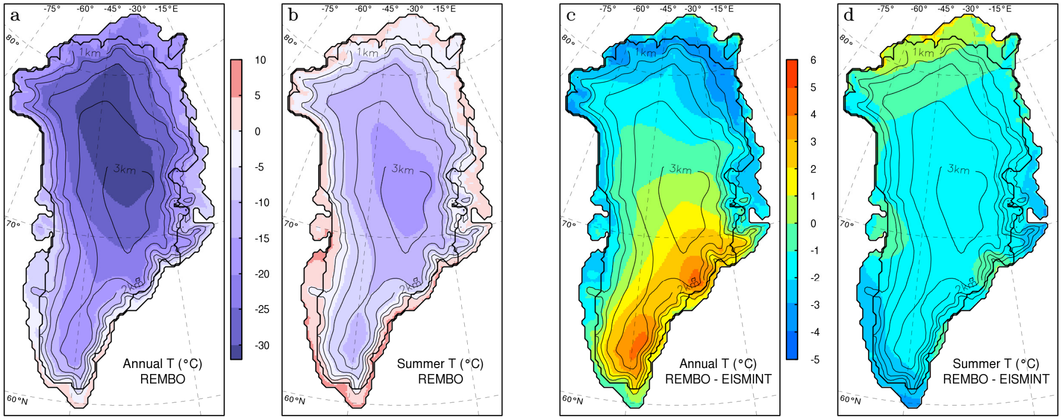

Fig. 3. REMBO model output of **(a)** mean annual temperature and **(b)** mean summer (JJA) temperature. Difference between REMBO and EISMINT for **(c)** mean annual temperature and **(d)** mean summer (JJA) temperature.

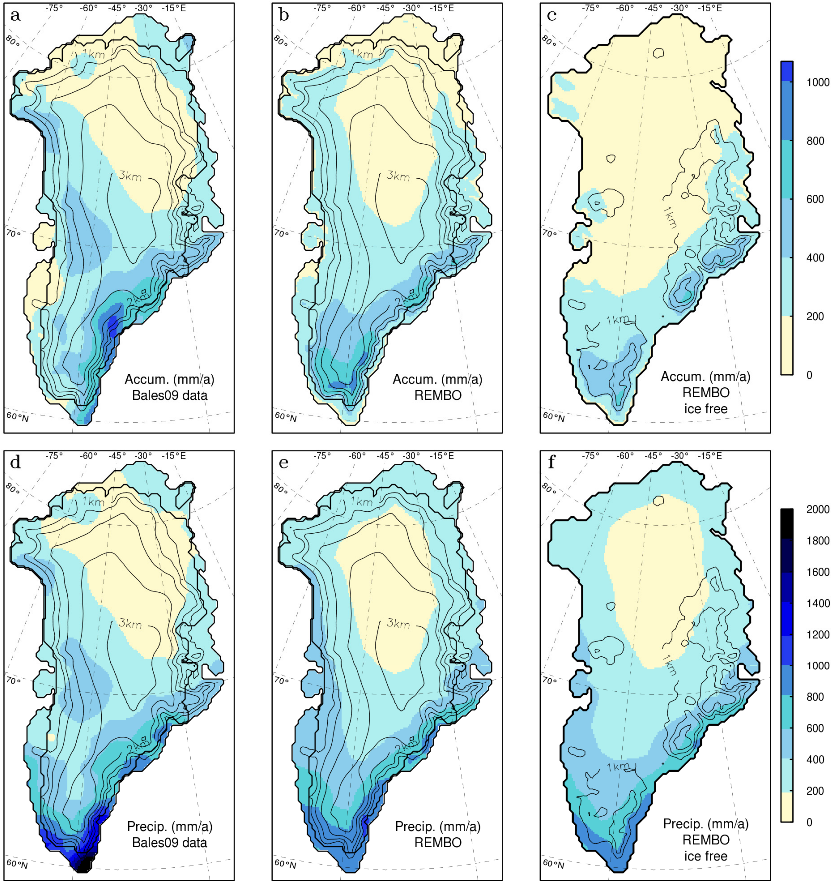

Fig. 4. Greenland accumulation fields from **(a)** present-day data, **(b)** REMBO for present-day topography and **(c)** REMBO for ice-free, uplifted bedrock topography. Total precipitation fields for the same are shown in **(d)**, **(e)** and **(f)**, respectively.

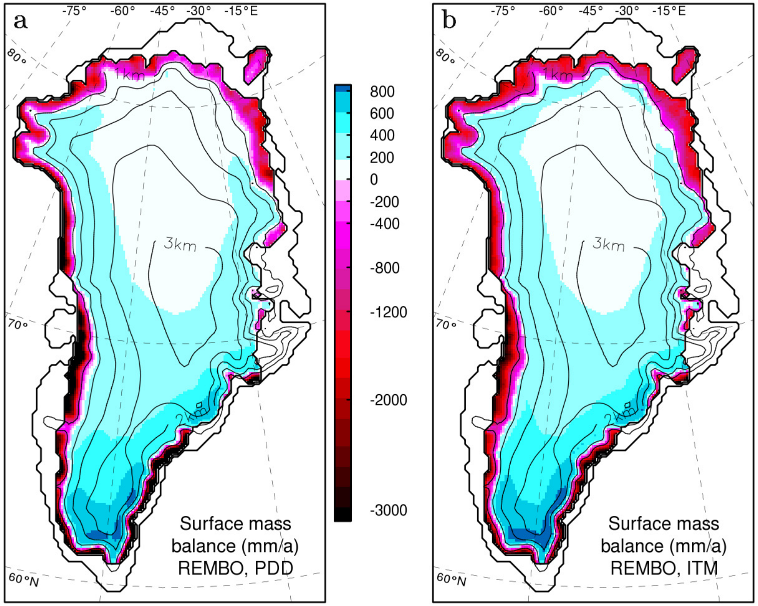

Fig. 5. Diagnosed surface mass balance for fixed, present-day topography using REMBO with ablation determined by **(a)** PDD and **(b)** ITM.

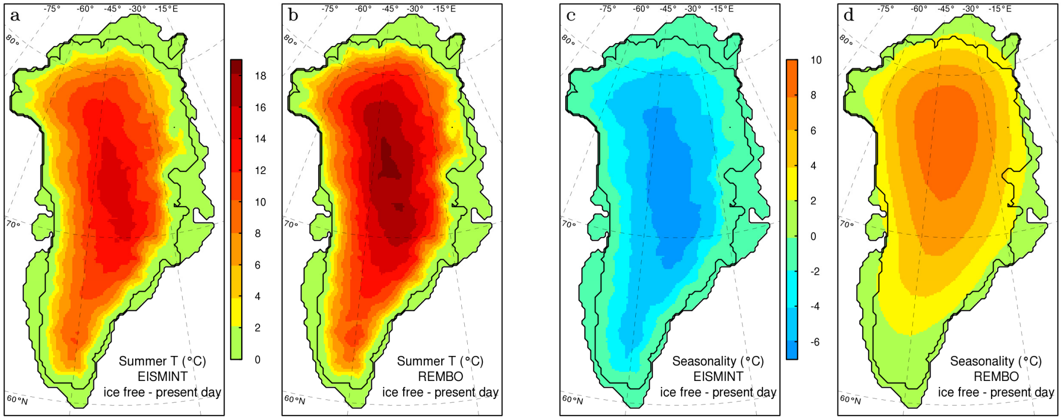

Fig. 6. Summer (JJA) temperatures for ice-free, uplifted bedrock topography minus those of present-day conditions for **(a)** the EISMINT temperature parameterization and **(b)** REMBO. Difference in seasonality (Jun-Jul-Aug temperature minus December-January-February temperature) for the uplifted, ice-free topography compared to present-day conditions using (a) the EISMINT temperature parameterization and (b) REMBO.

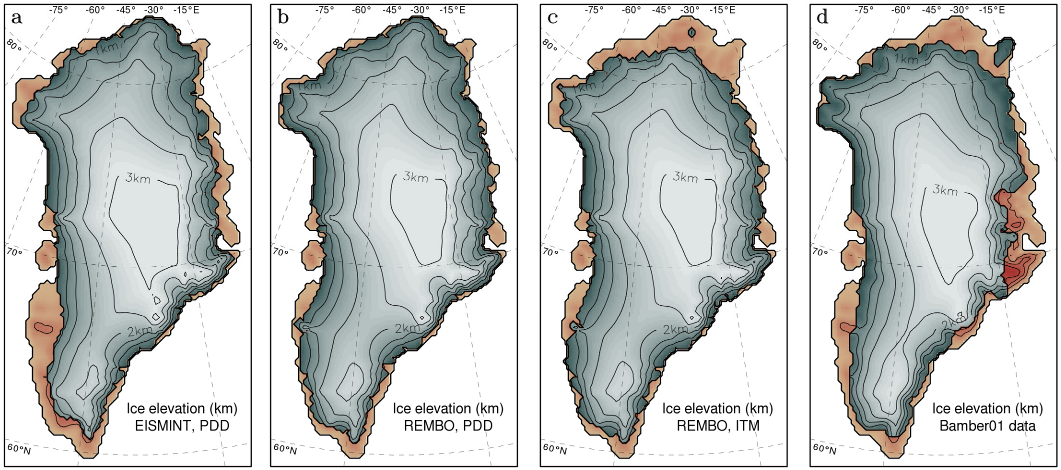

Fig. 7. Equilibrium simulated GIS elevations starting from present-day topography using **(a)** EISMINT with PDD ablation, **(b)** REMBO with PDD ablation, and **(c)** REMBO with ITM ablation, compared with **(d)** the actual GIS elevation from observations.

TCD
3, 729–764, 2009

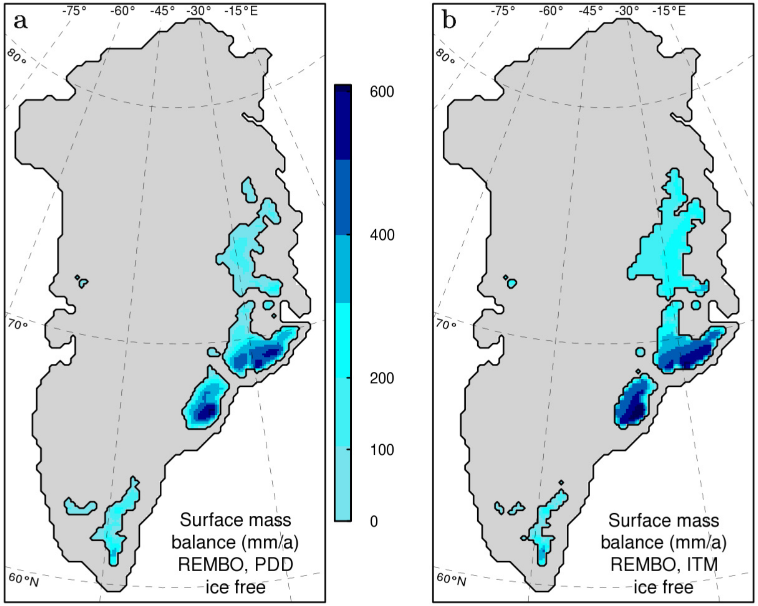

Fig. 8. Diagnosed area of positive surface mass balance for ice-free, uplifted bedrock topography using REMBO with ablation determined by **(a)** PDD and **(b)** ITM.

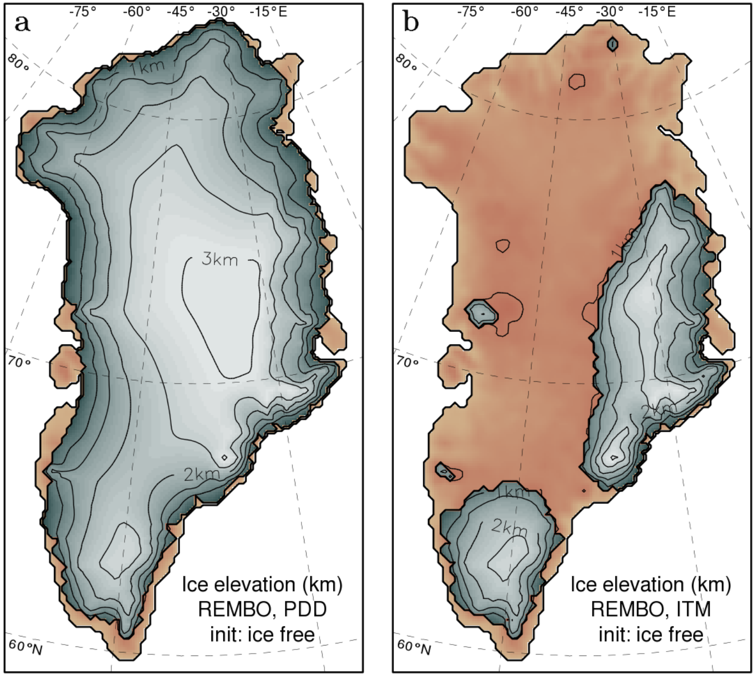

Fig. 9. Equilibrium simulated GIS elevation starting from ice-free, uplifted topography using REMBO with ablation determined by **(a)** PDD and **(b)** ITM.